The Role of a Microscopic Colloidally Stabilized Phase in Solubilizing Oligoamine-Condensed DNA Complexes

Vladimir S. Trubetskoy,* Jon A. Wolff,† and Vladimir G. Budker†
*Mirus Corporation, Madison, Wisconsin 53719; and †Departments of Pediatrics and Medical Genetics, Waisman Center, University of Wisconsin, Madison, Wisconsin 53705

ABSTRACT DNA complexes of spermine and spermidine become resolubilized at very high concentrations of the oligoamine. It has been postulated that high oligoamine concentrations shift the DNA from the globule back to the coil phase. The present study indicates that DNA resolubilization at high concentrations of spermine and spermidine is explained by formation of small particles of condensed DNA that cannot be precipitated by centrifugation. The fact that DNA stays condensed during resolubilization was confirmed using a relatively new condensation assay and three independent microscopic techniques. A considerable portion of DNA was found to be in particles with diameter <100 nm. Formation of such small particles is likely to be caused by colloidal forces. The ability to form small, condensed DNA particles in solutions that contain high concentrations of oligocation should aid in the design of synthetic DNA vectors for gene transfer and gene therapy and in the handling of DNA for diagnostic studies.

INTRODUCTION

The phenomenon of DNA condensation by multivalent oligoamines (such as spermine and spermidine) is of importance in such diverse fields as cell biology and materials science. Inquiry into this phenomenon presents the opportunity to model DNA packaging in nuclei and virions as well as to design new synthetic vectors for gene-transfer applications. A remarkable feature of oligoamine-condensed DNA is the ability to assume condition-defined morphologies such as spheroids, toroids, and rods (Bloomfield, 1996).

The theory of counterion condensation, developed by Manning (Manning, 1978) and experimentally proven by Wilson and Bloomfield with phage T7 DNA and spermidine (Wilson and Bloomfield, 1979), predicts the collapse of the DNA double-helix backbone when 90% of the phosphate charges are neutralized by counterion. The mechanism of this collapse is explained by attraction forces that are caused by correlated fluctuations of the counterion cloud that surrounds DNA and by hydration forces caused by the counterion-induced restructuring of water molecules between adjacent DNA strands (Bloomfield, 1996; Rouzina and Bloomfield, 1996).

One intriguing aspect of oligoamine DNA condensation is related to reports that DNA precipitates of spermine or spermidine dissolve at higher concentrations of the respective oligoamine (Pelta et al., 1996a, 1996b). Experimentally, this was based upon centrifugation and light-scattering studies. Nguyen et al. (2000) have postulated that solubilization of DNA/oligoamine condensates results from a sharp phase transition that occurs at a critical concentration that is related to the type of oligoamine. At this concentration, complete decondensation of DNA is postulated to be due to the screening of its charges by small polyamines and the eventual reversal of its charge from negative to positive (Nguyen et al., 2000).

Using a recently developed DNA condensation assay, the present study found that DNA remained condensed at the higher oligoamine concentrations that are associated with solubilization. Dynamic light-scattering (particle sizer), atomic force microscopy (AFM), and electron microscopy (EM) studies indicate that solubilization is also accompanied by a dramatic reduction in particle size. In addition, DNA containing covalently attached gold particles was used for the first time to demonstrate DNA compaction on EM images. The implications of these observations are discussed in terms of colloidal forces.

MATERIALS AND METHODS

Materials

All condensation and resolubilization experiments were performed using pCILuc plasmid DNA (Zhang et al., 1997). Spermine and spermidine were purchased from Aldrich (Milwaukee, WI). Penta-L-lysine ($(Lys)_5$) and deca-L-lysine ($(Lys)_{10}$) oligopeptides were synthesized using a model 433A peptide synthesizer (Applied Biosystems) and were purified using high-performance liquid chromatography.

DNA labeling with fluorescent moieties

Covalent labeling of plasmid DNA with fluorophores was performed using tetramethylrhodamine (TMR) LabelIT reagent (Mirus Corp., Madison, WI) as previously described (Trubetskoy et al., 1999). Briefly, plasmid DNA and a solution of LabelIT reagent in methyl sulfoxide (100 mg/ml) were mixed in 1 ml of 10 mM HEPES, pH 7.5 at a reagent/DNA ratio of 5:1 (w/w). The reaction mixture was incubated for 1 h at 37°C. Labeled DNA was then precipitated three times in 70% ethanol with 0.2 M NaCl. Three or four TMR labels were consistently introduced per 100 basepairs of the plasmid DNA as was determined by spectrophotometry at 555 and 260 nm. As judged from agarose gel electrophoresis, no plasmid degradation was detected after the labeling (results not shown).

Submitted July 8, 2002, and accepted for publication October 18, 2002.
Address reprint requests to Dr. Vladimir S. Trubetskoy, Mirus Corp., 505 S. Rosa Rd., Madison, WI 53719. Tel.: 608-441-2832; Fax: 608-441-2849; E-mail: vladimirt@genetransfer.com.

0006-3495/03/02/1124/07 $2.00

DNA condensation assay

The collapse of TMR-labeled DNA was assessed using a quantitative assay based on condensation-induced quenching of a fluorophore covalently attached to DNA (Trubetskoy et al., 1999). Because only 3 or 4 fluorophores per 100 basepairs were covalently attached to the DNA, it was expected that increasing the oligoamine concentration would only slightly affect its DNA binding. In contrast, the commonly used ethidium bromide assay suffers from the ability of the oligoamine to inhibit DNA binding of the cationic ethidium bromide.

Briefly, TMR-DNA (10 μg) was mixed with various quantities of either spermidine or spermine in 0.5 ml of 10 mM HEPES, pH 7.5. Stock solutions of the oligoamines were titrated to pH 7.5. After incubation for 10 min at room temperature, TMR fluorescence of the samples was measured using a Shimadzu RF 1501 spectrofluorometer (excitation wavelength (λ_{ex}) of 555 nm; emission wavelength (λ_{em}) of 585 nm) at room temperature. Relative signal was calculated as the percentage of fluorescence of noncondensed TMR-DNA. As controls, equivalent amounts of TMR-LabelIT were incubated with the same concentrations of the oligoamines.

AFM

Images of oligoamine-condensed DNA particles were obtained using a Dimension 3100 AFM microscope (Digital Instruments, Santa Barbara, CA). Unlabeled plasmid DNA was condensed in 150 mM spermine, pH 7.5. The complex was centrifuged for 7 min at 11,000 *g* in a microcentrifuge. DNA solution (2 μg/ml) was incubated on the surface of a freshly cleaved mica disk for 10 min at room temperature. The excess of liquid was removed by a stream of nitrogen and then imaged in the air using the noncontact mode within 1 h after deposition on mica.

Particle sizing

The size of the DNA/oligoamine complexes were measured using a Zeta Plus particle sizer (Brookhaven Instruments, Holtsville, NY). Unlabeled plasmid DNA (10 μg) was mixed with corresponding amounts of oligoamines and was measured after 10 min of incubation at room temperature. Stock solutions of oligoamines were titrated to pH 7.5 and centrifuged at 20,000 *g* for 10 min to remove unsoluble particulates that interfered with particle-size measurements.

Complex precipitation in a microfuge

In addition to the particle sizing, the resolubilization of DNA/spermine complexes was studied by DNA precipitation in a microfuge under the conditions described by Pelta et al. (1996b). Briefly, unlabeled DNA (10 μg) was mixed with a corresponding amount of spermine (pH 7.5), incubated for 15 min at room temperature, and centrifuged at 11,000 *g* for 7 min. The amount of DNA in the precipitate was calculated by subtracting the ultraviolet (UV) spectra of the complexes before and after centrifugation. To exclude the light-scattering share for the optical density at 260 nm (OD_{260}) values of the DNA/spermine complexes, the following formula has been used:

$$OD_{260,correct} = (OD_{260} - OD_{230}) \times 2,$$

where OD_{230} is the optical density at 230 nm. This formula takes advantage of the fact that for pure DNA, $OD_{260} = 2 \times OD_{230}$ (Manchester, 1996).

Covalent labeling of plasmid DNA with Nanogold particles

Plasmid DNA was covalently labeled with pyridyldithio (PDP)-cysteine-LabelIT reagent (Mirus Corp.). The reagent was mixed with the DNA in 10 mM HEPES, pH 7.5 at a 0.1:1 reagent/DNA ratio (w/w) and was incubated for 1 h at 37°C. Labeled DNA was purified from the excess of the reagent by repeating the precipitation in a solution of 70% ethanol with 0.3 M NaCl. PDP-DNA (200 μg in 200 μl of 10 mM MOPS, pH 6.5) was incubated with 1 mM of Tris(2-carboxyethyl)phosphine (Pierce, Rockford, IL) for 10 min at room temperature to reduce PDP residues on the DNA. Monomaleimido Nanogold labeling reagent (30 μl of 100 μM stock solution; Nanoprobes, Yaphank, NY) was added to the modified plasmid. The reaction mixture was incubated for 24 h at 4°C. Gold-labeled DNA was separated from the excess of the gold reagent using a Sepharose 4B-CL column (10 × 0.5 cm). The labeling resulted in ~40 gold clusters per plasmid (as determined from OD_{260} and OD_{420} measurements of the purified conjugate, according to Nanoprobes instructions).

EM of DNA/spermine and gold-labeled DNA/spermine condensates

The complexes of nonlabeled and gold-labeled plasmid DNA in 150 mM spermine, pH 7.5 (10 μg of DNA/ml) were incubated directly on glow-discharged Formvar-coated nickel grids (400 mesh) for 5 min at room temperature. In the case of nonlabeled DNA, after the excess of the solution was blotted with filter paper, the grids were treated with 1% neutralized uranyl acetate solution for 30 s. In the case of gold-labeled DNA, the grids were extensively washed with Milli-Q water and were treated with HQ silver-enhancement reagent (Nanoprobes) for 4 min at room temperature.

For noncondensed, gold-labeled DNA viewing, the grids were treated with poly-L-lysine solution (10 μg/ml, mol wt 30 kDa; Sigma, St. Louis, MO) for 5 min at room temperature, washed with Milli-Q water, and then incubated with gold-labeled plasmids (10 μg/ml) for another 5 min. Silver enhancement was performed as described for spermine-condensed samples. All samples then were viewed using a Phillips SM 120 transmission electron microscope.

RESULTS

Particle sizing and DNA condensation studies

We confirmed that an increasing spermine or spermidine concentration can solubilize the respective DNA/oligoamine mixtures. On the basis of dynamic light-scattering analysis (using the particle sizer), this was accompanied by a dramatic decrease in DNA complex size when the oligoamine concentration was increased to ~100 mM (Fig. 1). At the highest concentration of 200 mM, the DNA/oligoamine complexes decreased to 200–300 nm on average. The shape of the correlation function indicated a broad size distribution (data not shown).

Particle-size measurements were correlated with the outcome of microfuge precipitations that were carried out under conditions described by Pelta et al. (1996b). Although some discrepancies between particle sizing and precipitation were observed in the 0.05–0.5 mM range of spermine concentrations (Fig. 2), a significant degree of correlation was achieved, especially in the region of our particular interest (>100 mM). Control sizing of the uncondensed plasmid at 20 μg/ml was not performed due to insufficient light scattering.

The extent of DNA condensation at solubilizing concentrations of spermine or spermidine was determined using DNA covalently labeled with TMR groups. When the DNA

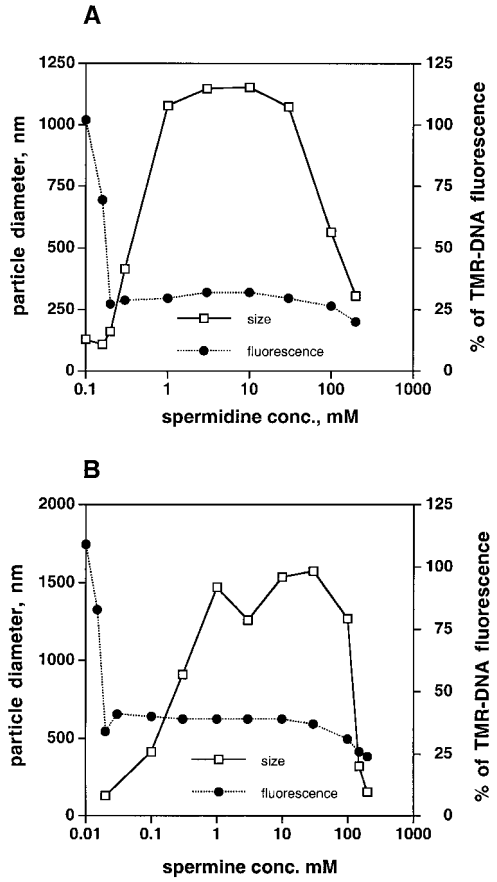

FIGURE 1 Dependence of DNA condensation and DNA/polyamine complex diameter on the concentration of spermidine (*A*) or spermine (*B*). Ten micrograms of unlabeled DNA (for particle sizing) or TMR-DNA (for condensation) were mixed with various amounts of polyamine stock solutions that had been titrated to pH 7.5 and incubated for 10 min before measurement of fluorescence or sizing. All samples were diluted to the equal volume of 0.5 ml with 10 mM HEPES, pH 7.5. DNA condensation was assessed by a decrease in TMR-DNA fluorescence, and particle diameter was determined by dynamic light scattering.

condenses and undergoes a coil-globule transition, the covalently attached fluorescent labels become concentrated and self-quench (Trubetskoy et al., 1999). A fourfold decrease in TMR fluorescence was observed with DNA collapse upon electrostatic interaction with the oligoamines. The minimum oligoamine concentration required for DNA collapse was 0.2 mM for spermidine and 0.02 mM for spermine. In contrast to what we expected based upon the literature (Nguyen et al., 2000), TMR-DNA fluorescence did not increase at the solubilizing concentrations of the oligoamines. Instead, we observed a slight decrease in fluorescence, which suggests additional compaction of the plasmid (Fig. 1). In a control experiment, the fluorescence levels of hydrolyzed TMR-LabelIT reagent alone were unchanged after being mixed with the same concentrations of oligoamines, which indicates that the observed fluorescence decrease was associated with DNA collapse and was

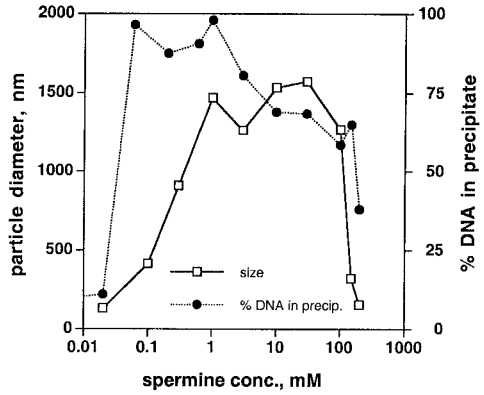

FIGURE 2 Comparison of particle sizing of the DNA/spermine complexes from Fig. 1 *B* with precipitation of the same complexes in a microcentrifuge performed under the conditions described by Pelta et al. (1996b). Conditions of the experiment were the same as described for Fig. 1.

not due to the quenching of TMR by the oligoamine itself (data not shown). Thus, our fluorescence studies indicate that DNA remains in a compacted form when it is solubilized.

AFM and EM studies

To confirm our findings using another methodology, we probed DNA/oligoamine condensates using various microscopic methods. For AFM, the DNA/spermine complexes (2 μg/ml of plasmid in 150 mM spermine, pH 7.5) were deposited directly on the surface of negatively charged mica disks and then scanned in noncontact mode. Spherical compact particles with a wide variety of sizes (some of them $<$100 nm in diameter) were detected (Fig. 3 *A*), thus corroborating the particle-sizing data.

The same DNA/spermine mixture was also examined using two independent transmission EM techniques. We studied the complexes contrasted with 1% uranyl acetate and the complexes in which the DNA was covalently labeled with electron-dense gold nanoparticles. Both methods yielded surprisingly similar results, which were in turn similar to the AFM data described. Low-magnification field views for both methods produced images of spherical DNA particles with a broad range of sizes including significant numbers of very small ones (Fig. 3, *B* and *E*).

Explicitly, uranyl acetate enhancement resulted in negative DNA contrast (DNA particles in white on a black background) on transmission EM images that is characteristic for cation-condensed DNA structures where a contrasting stain fails to intercalate inside the double helix that outlines the condensed aggregate as a whole (Ghirlando et al., 1992). In addition to highly condensed DNA/spermine structures, less-condensed positively contrasted areas were also observed (Fig. 3 *C*, *arrowhead*).

Although uranyl acetate usually does not alter the morphology and state of condensation of the substrate-bound DNA, it could, because it has been shown to be a very

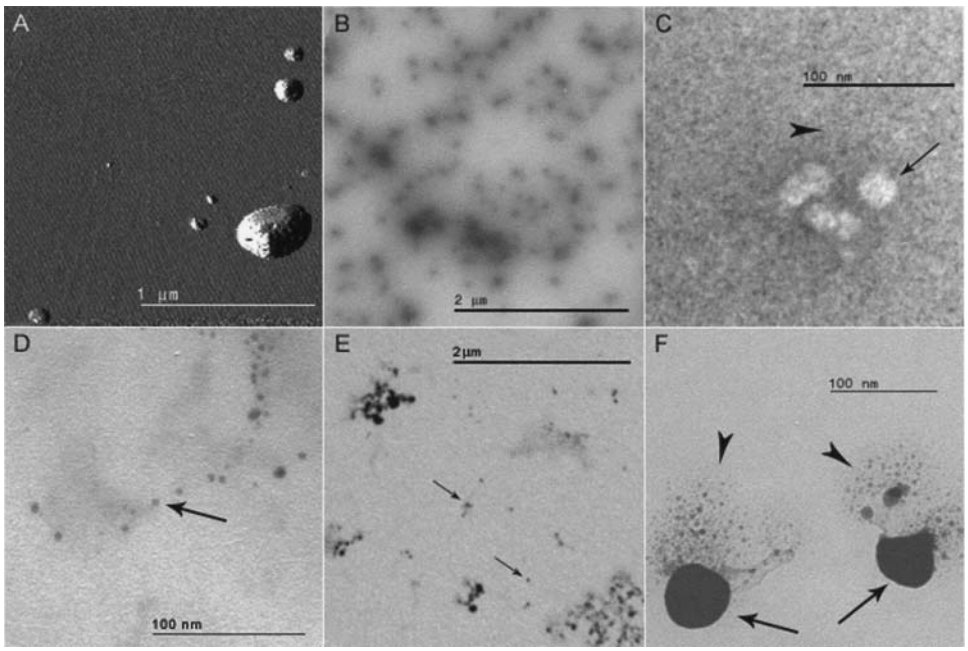

FIGURE 3 Microscopic studies of DNA and gold-DNA condensates in 150 mM spermine. (*A*) AFM image of unlabeled DNA/spermine complex. (*B, C*) EM images of the unlabeled DNA complexes enhanced with 1% uranyl acetate viewed under low and high magnifications, respectively. Arrow, small particle of uranyl acetate-impermeable condensed DNA; arrowhead, ''spillage'' of the less-condensed complex on the substrate. (*D*) EM with gold-DNA conjugate: noncondensed gold-DNA on poly-L-lysine-coated substrate. Arrow, string of silver-enhanced gold particles along the poly-L-lysine-adsorbed plasmid. (*E, F*) EM with gold-DNA conjugate: gold-DNA/spermine complexes shown under low and high magnifications, respectively. In part *E*, arrows indicate individual small particles; in *F*, arrows show silver-enhanced highly condensed parts, and arrowheads indicate spillage of the less-condensed complex on the substrate.

strong condensing agent for the DNA in solution (Cherny and Jovin, 2001). To exclude this possible interference, we used another transmission EM method that is based on the direct covalent labeling of plasmid DNA with electron-dense gold nanoparticles. This covalent conjugate was prepared using the PDP-cysteine-LabelIT reagent (Mirus Corp.) and the monomaleimido Nanogold labeling reagent (Nanoprobes). Because Nanogold reagents are very small gold clusters (1.4 nm in diameter) that are difficult to view using conventional transmission EM techniques, the silver-enhancement procedure recommended by the Nanoprobes company was used. This procedure results in electron-dense gold or silver particles with average diameter of 3–10 nm, depending on the time of the incubation with silver reagent. Fig. 3 *D* shows a silver-enhanced image of a noncondensed (stretched) gold-labeled plasmid adsorbed on a poly-L-lysine-covered grid. Characteristic ''bead-on-the-string'' structures that outlined extended strands of plasmid DNA were evident (Fig. 3 *D*, *arrow*). However, quite different structures were observed in silver-enhanced images of gold-DNA in 150 mM spermine (Fig. 3, *E* and *F*). In these compacted DNA structures, silver enhancement may cover the condensed complex so as to obscure individual gold or silver grains. High-magnification images of such small particles show areas of complete silver enhancement that are related to the highly condensed parts of the complex (Fig. 3 *F*, *arrows*) and ''spillage'' of gold-labeled DNA strands on the substrate (Fig. 3 *F*, *arrowheads*). This spillage likely results from the interaction of the positively charged complex with the negatively charged substrate coating.

Therefore, the microscopic examination of the DNA and gold-DNA mixtures with 150 mM spermine confirmed the sizing results of their dynamic light scattering: at this concentration of the oligoamine, a significant decrease in the sizes of condensed DNA complexes can be observed. However, no microscopic evidence of DNA decondensation in 150 mM spermine solution was detected. All DNA apparently was associated with the condensed structures, and no decondensed DNA morphologies (similar to what is depicted in Fig. 3 *D*) were observed.

Oligolysine studies

We hypothesized that the ability of an oligocation to solubilize condensed DNA complexes is similar to the phenomenon of DNA/polycation condensation and, therefore, should be dependent on the number of positive charges carried by the oligocation (see Discussion). To address this question, $(Lys)_5$ and $(Lys)_{10}$ were complexed with DNA under the same conditions used for the spermidine and spermine studies, and the sizes of the DNA particles were determined (Fig. 4). Fig. 4 depicts the complex size measured by dynamic light scattering as a function of molar concentration of positive charges for each oligolysine (assuming 6 charges for $(Lys)_5$ and 11 charges for $(Lys)_{10}$). Solubilization of the complexes was observed for both oligolysines, and the degree of solubilization was indeed dependent on the number of charges each contained. $(Lys)_{10}$ was able to solubilize DNA at a significantly lower concentration of positive charges (0.1 mM) than the shorter $(Lys)_5$ (~10 mM). In terms of the positive-to-negative charge ratio, solubilization of DNA with $(Lys)_{10}$ and $(Lys)_5$ required 160 and 8000 times the positive charge excess, respectively.

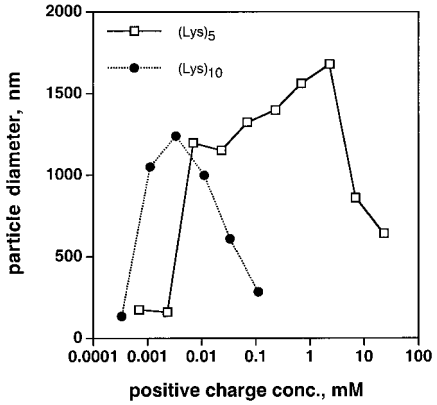

FIGURE 4 The size of DNA/oligolysine complexes measured using dynamic light scattering in dependence of molar positive-charge concentrations. DNA (10 μg in 0.5 ml of 10 mM HEPES, pH 7.5) was incubated with corresponding concentrations of $(Lys)_5$ and $(Lys)_{10}$ for 10 min at room temperature before measurements.

DISCUSSION

The relationship between aggregation and condensation upon interaction of DNA with polyamines is still a matter of debate. Some authors associate DNA condensation with aggregation, arguing that these two phenomena are hard to distinguish (Bloomfield, 1996; Raspaud et al., 1998). Others maintain that this is true only for short DNA molecules (shorter than several hundred basepairs; Yoshikawa, 2001). Collapse of the individual large DNA molecules without aggregation was detected only at extremely low DNA concentrations (usually <0.5 μg/ml (Porschke, 1984; Widom and Baldwin, 1983)). At higher DNA concentrations, addition of polyamine always resulted in aggregation regardless of the length of the DNA molecule.

In this context, the recently reported DNA/polyamine solubilization phenomenon has sparked further interest in this issue. Theoretical explanation of the complex solubilization involves charge reversal of the complexes and DNA decondensation (Nguyen et al., 2000). The authors build a theoretical model in which solubilization causes the DNA to undergo complete charge reversal and exist in its expanded-coil (decondensed) conformation. The existence of a globule-coil phase transition during solubilization was expressly stated in this model (Nguyen et al., 2000).

Contrary to these notions, our results indicate that the solubilization of DNA/oligoamine condensates at high oligoamine concentrations results from the formation of colloidally stable small particles of condensed DNA. Our condensation assay using DNA covalently labeled with a fluorescent probe (Fig. 1) clearly demonstrated that DNA remains condensed under solubilization conditions for both spermine and spermidine (Trubetskoy et al., 1999). A variety of microscopic methods were used to further investigate the state of DNA in 150 mM spermine solution. Such methods included AFM of DNA/spermine complexes directly adsorbed on mica, two independent transmission EM methods that employed DNA contrasted with uranyl acetate, and silver-enhanced transmission EM of the complexes prepared with gold-labeled DNA. All microscopic studies confirmed the results obtained using particle sizing: DNA in 150 mM spermine formed complexes with a broad size distribution including very small (<100 nm in diameter) particles (Fig. 3, *C* and *F*). Negative uranyl acetate contrast of such particles in EM images indicated that the DNA was condensed, which confirms the results obtained with fluorescence quenching. AFM also was able to distinguish between completely condensed, partially condensed, and noncondensed plasmid DNA (Fang and Hoh, 1998; Hansma et al., 1998). Neither noncondensed nor partially condensed morphologies were observed in our AFM studies. Of course, it is difficult to quantify the percentage of collapsed versus noncondensed DNA species using any of the above microscopy methods. However, to demonstrate that the resolubilization of DNA/spermine condensates at high oligoamine concentrations is not caused by decondensation, it is enough to show that supernatants after centrifugation still contain some condensed forms.

The data indicate that a globule-coil phase transition does not occur upon DNA solubilization in high spermidine or spermine concentrations. The DNA forms the same condensed phase, only it is more finely dispersed. Formation of smaller particles helps in avoiding DNA precipitation during centrifugation, which has been the major experimental criterion of polyamine-induced solubilization (Raspaud et al., 1998).

DNA complexes with larger, water-soluble polycations such as poly-L-lysine also form small particles of condensed DNA that are resistant to precipitation upon centrifugation when a charge excess of polycation is mixed with DNA at a low DNA concentration (typically <0.1 mg of DNA/ml) and in aqueous solution containing little or no salt (Tang and Szoka, 1997; van de Wetering et al., 1998; Wolfert et al., 1996). In such precipitation-resistant complexes, the DNA is condensed within particles that have a diameter <100 nm. This conclusion is based on the combination of different physicochemical methods. The complex size was usually confirmed using dynamic light scattering (Pouton et al., 1998; van de Wetering et al., 1998) or various microscopic methods (Hansma et al., 1998; Kwoh et al., 1999; Martin et al., 2000; Tang and Szoka, 1997; Wolfert et al., 1996). In addition to these microscopy methods, the proof that DNA is condensed could be obtained by fluorescence methods: either by cation-mediated exclusion of ethidium bromide (Pouton et al., 1998; Tang and Szoka, 1997; van de Wetering et al., 1998) or by the fluorescence decrease of the fluorophore-DNA conjugate upon addition of a cation (Trubetskoy et al., 1999).

Similar particles are obtained not only for DNA serving as the polyanion, but for any polyanion or polycation interpolyelectrolyte complex formed from two polyelectrolytes

of opposite charge in a low-monovalent-salt aqueous solution. If one of them is in excess (positive/negative charge ratio $\neq 1$), they form colloidally stable nonflocculated complexes that possess a surface charge of the same sign as the excess polyion (Pogodina and Tsvetkov, 1997).

This last observation on ζ-potential helps to relate polycation DNA complexes to solubilized DNA/spermine particles. It is well known that all surface potentials, including the experimentally measurable ζ-potential, diminish sharply with increasing ionic strength of the bulk solution (Shaw, 1991). Because the ionic strength of spermine solution at 100 mM might exceed 1.8 M (assuming the spermine charge at pH 7.4 to be 3.8 (Geall et al., 2000)), the ζ-potential can be very difficult to measure under these conditions. We hypothesize that charge reversal is confined only to the surface of the complexes and serves as a driving force for the dispersion of the precipitate. The dispersion of DNA/polyamine condensates can be explained by the colloid electrostatic stabilization (i.e., confined only to the particle interface) and can be induced by a condition known in colloid chemistry as peptization. Peptization is defined as dispersion achieved by changing the composition of the dispersion medium and frequently includes the addition of polyvalent co-ions (Shaw, 1991). In our particular case, oligoamines serve simultaneously as particle-forming (condensing) agents at lower concentrations and peptization (dispersion) agents at higher concentrations.

The oligolysine experiment further relates the colloidal nature of the solubilization phenomenon with properties of DNA/polyamine complexes (Fig. 4). An increase in the number of charges on the condensing and dispersing cation narrowed the polyamine concentration range wherein DNA is insoluble. Going from 6 to 11 positive charges on a polyamine resulted in a decrease in the ''insolubility concentration range'' by several orders of magnitude (Fig. 4). The use of polylysine as a DNA condensing agent with hundreds of positive charges decreases the precipitation range further (Lee and Huang, 1996). Thus, the colloidal processes involved in the formation of soluble DNA complexes with either oligocations or polycations are basically the same.

In summary, several independent methods indicate that globule-coil phase transition is an unlikely event during the solubilization of DNA at high oligoamine concentrations, and the DNA remains condensed. Solubilization can be explained by the significant decrease in condensed DNA particle size, which is likely caused by colloidal forces. The ability to form small, condensed DNA particles in solutions that contain high concentrations of oligocation should aid in the design of synthetic DNA vectors for gene therapy and in the handling of DNA for diagnostic studies.

REFERENCES

Bloomfield, V. A. 1996. DNA condensation. *Curr. Opin. Stuct. Biol.* 6:334–341.

Cherny, D. I. and T. M. Jovin. 2001. Electron and scanning force microscopy studies of alterations in supercoiled DNA tertiary structure. *J. Mol. Biol.* 313:295–307.

Fang, Y. and J. H. Hoh. 1998. Early intermediates in spermidine-induced DNA condensation on the surface of mica. *J. Am. Chem. Soc.* 120: 8903–8909.

Geall, A. J., R. J. Taylor, M. E. Earll, M. A. Eaton, and I. S. Blagbrough. 2000. Synthesis of cholesteryl polyamine carbamates: Pk(a) studies and condensation of calf thymus DNA. *Bioconjug. Chem.* 11:314–326.

Ghirlando, R., E. J. Wachtel, T. Arad, and A. Minsky. 1992. DNA packaging induced by micellar aggregates: a novel in vitro DNA condensation system. *Biochemistry* 31:7110–7119.

Hansma, H. G., R. Golan, W. Hsieh, C. P. Lollo, P. Mullen-Ley, and D. Kwoh. 1998. DNA condensation for gene therapy as monitored by atomic force microscopy. *Nucleic Acids Res.* 26:2481–2487.

Kwoh, D. Y., C. C. Coffin, C. P. Lollo, J. Jovenal, M. G. Banaszczyk, P. Mullen, A. Phillips, A. Amini, J. Fabrycki, R. M. Bartholomew, S. W. Brostoff, and D. J. Carlo. 1999. Stabilization of poly-L-lysine/DNA polyplexes for in vivo gene delivery to the liver. *Biochim. Biophys. Acta* 1444:171–90.

Lee, R. J. and L. Huang. 1996. Folate-targeted, anionic liposome-entrapped polylysine-condensed DNA for tumor cell-specific gene transfer. *J. Biol. Chem.* 271:8481–8487.

Manchester, K. L. 1996. Use of UV methods for measurement of protein and nucleic acid concentrations. *Biotechniques* 20:968–970.

Manning, G. S. 1978. The molecular theory of polyelectrolyte solutions with applications to the electrostatic properties of polynucleotides. *Q. Rev. Biophys.* 11:179–246.

Martin, A. L., M. C. Davies, B. J. Rackstraw, C. J. Roberts, S. Stolnik, S. J. Tendler, and P. M. Williams. 2000. Observation of DNA-polymer condensate formation in real time at a molecular level. *FEBS Lett.* 480:106–112.

Nguyen, T. T., I. Rouzina, and B. I. Shklovski. 2000. Reentrant condensation of DNA induced by multivalent counterions. *J. Chem. Phys.* 112:2562–2568.

Pelta, J., Jr., D. Durand, J. Doucet, and F. Livolant. 1996a. DNA mesophases induced by spermidine: structural properties and biological implications. *Biophys. J.* 71:48–63.

Pelta, J., F. Livolant, and J. L. Sikorav. 1996b. DNA aggregation induced by polyamines and cobalthexamine. *J. Biol. Chem.* 271:5656–5662.

Pogodina, N. V. and N. V. Tsvetkov. 1997. Structure and dynamics of the polyelectrolyte complex formation. *Macromolecules* 30:4897–4904.

Porschke, D. 1984. Dynamics of DNA condensation. *Biochemistry* 23:4821–4828.

Pouton, C. W., P. Lucas, B. J. Thomas, A. N. Uduehi, D. A. Milroy, and S. H. Moss. 1998. Polycation-DNA complexes for gene delivery: a comparison of the biopharmaceutical properties of cationic polypeptides and cationic lipids. *J. Control. Release* 53:289–299.

Raspaud, E., M. Olvera de la Cruz, J. L. Sikorav, and F. Livolant. 1998. Precipitation of DNA by polyamines: a polyelectrolyte behavior. *Biophys. J.* 74:381–393.

Rouzina, I. and V. A. Bloomfield. 1996. Macroion attraction due to electrostatic correlation between screening counterions. I: mobile surface-adsorbed ions and diffuse ion cloud. *J. Phys. Chem.* 100: 9977–9989.

Shaw, D. J. 1991. Colloid and surface chemistry: Butterworth-Heinemann Oxford.

Tang, M. X., and F. C. Szoka, Jr. 1997. The influence of polymer structure on the interactions of cationic polymers with DNA and morphology of the resulting complexes. *Gene Ther.* 4:823–832.

Trubetskoy, V. S., P. M. Slattum, J. E. Hagstrom, J. A. Wolff, and V. G. Budker. 1999. Quantitative assessment of DNA condensation. *Anal. Biochem.* 267:309–313.

van de Wetering, P., J. Y. Cherng, H. Talsma, D. J. Crommelin, and W. E. Hennink. 1998. 2-(dimethylamino)ethyl methacrylate based (co)polymers as gene transfer agents. *J. Control. Release.* 53:145–153.

Widom, J., and R. L. Baldwin. 1983. Monomolecular condensation of lambda DNA induced by cobalthexamine. *Biopolymers*. 22: 1595–1620.

Wilson, R. W. and V. A. Bloomfield. 1979. Counterion-induced condensation of deoxyriobonucleic acid. A light scattering study. *Biochemistry* 18:2192–2196.

Wolfert, M. A., E. H. Schacht, V. Toncheva, K. Ulbrich, O. Nazarova, and L. W. Seymour. 1996. Characterization of vectors for gene therapy formed by self-assembly of DNA with synthetic block co-polymers. *Hum. Gene Ther*. 7:2123–2133.

Yoshikawa, K. 2001. Controlling the higher-order structure of giant DNA molecules. *Adv. Drug Deliv. Rev*. 52:235–244.

Zhang, G., D. Vargo, V. G. Budker, N. Armstrong, S. Knechtle, and J. A. Wolff. 1997. Expression of naked plasmid DNA injected into the afferent and efferent vessels of rodent and dog livers. *Hum. Gene Ther*. 8: 1763–1772.